Energy Conversion
Circuit Laboratory

Design of Fluorescent Lamp Ballast with PFC using a Power Piezoelectric Transformer

Sung-Jin Choi, Kyu-Chan Lee, and Bo H. Cho
The School of Electrical Engineering
Seoul National University
Seoul, Korea.

Abstract - **An investigation of a high power piezoelectric transformer as a potential component for a fluorescent lamp ballast with power factor correction (PFC) is discussed. The attractiveness of the piezoelectric transformer is primarily simplicity of the resulting circuit, and it is easy to be produced in mass with a low cost. Electrical modeling considering operating current level and analysis of the piezoelectric transformer are performed through measurements to design a fluorescent lamp ballast with a single stage charge pump PFC. The experimental and simulation results are provided to verify theoretical analysis.**

I. INTRODUCTION

The piezoelectric transformer (PT) is an electro-mechanical device that transfers electrical energy through a mechanical vibration. It features high voltage gain, high power density, compact size, and no electromagnetic noise. Since proposed by Rosen in the 1950s, quite a few papers have proposed the applications with different PTs[1]-[2]. Recently, the applications of PT have extended to the power level of 20W in DC-DC converters [3]-[6].

In this paper, a PT operating in the contour vibration mode is introduced for an application of fluorescent lamp ballast. Utilizing its inherent characteristics of the LC resonator and a high voltage gain to ignite the lamp in light load condition, FL ballast using the PT to eliminate the magnetic component is suggested. PT is easy to be produced in mass and reduces the cost of the ballast. When the PT is integrated into a single stage PFC fluorescent lamp ballast - the charge pump PFC circuit[7], the scheme reduces the number of components of the ballast circuit.

In section II, modeling of the PT taking into account of the operating current level is discussed. In section III, various ballast schemes employing the PT are presented. The experimental results are presented in section IV.

II. MODELING AND ANALYSIS OF PIEZOELECTRIC TRANSFORMER

Fig. 1 shows the structure of the PT used in this paper. The piezoelectric material is PZT (lead zirconate titanate) and it has a primary electrode in the center and a secondary in the outer part. It operates in the contour vibration mode and the mechanical resonant frequency is around 75kHz. It has the band pass characteristics and provides the high voltage gain in the light load condition.

An electrical equivalent circuit of the PT around the frequency range of interest can be represented by a well-known resonant band-pass circuitry as shown in Fig. 2 [8]. Its circuit parameter values are calculated through several 2-port measurement techniques – admittance circle measurement [9] and s-parameter measurement[10], which may be performed in the signal level.

To design the ballast circuit, the electrical equivalent circuit for the PT which calculates both the steady state and the starting voltage gain is needed. The electrical circuit model of PT is established in the several papers [8]-[10], but these models did not consider the mechanical quality factor variation as the input current level varies. Especially in the light load condition, there is too large error between measured and simulated data when signal level measurement

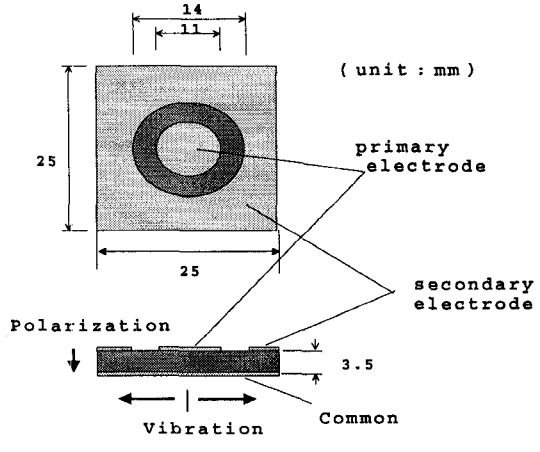

Fig. 1. 18W PT operating in the contour vibration mode (Korea Tronix sample)

This work was partially supported by Korea Tronix Co., Ltd.

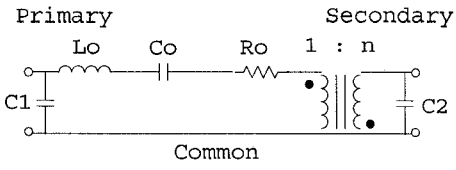

Fig. 2. Conventional circuit model of the PT around the resonant frequency

is used.

In general, the voltage gain of PTs decreases as the input current increases. It is because the mechanical quality factor (Qm) of the mechanical part of PTs is lowered, as the mechanical velocity of the surface increases. It is represented as a current (i_m) through the resonant branch in the mechanical part of the electrical equivalent model in Fig.3. This phenomenon can be modeled by replacing the constant internal resistance, Ro by the variable resistance, Rv as in Fig. 3. Rv describes the mechanical quality factor and is an increasing function of the current flow,

$$R_v = f(i_m) = \tilde{f}(i_0) \cong \hat{f}(i_1). \qquad (1)$$

The circuit parameters in the model for the PT are measured and calculated as follows: Lo = 103.8 mH, Co = 42.9 pF, C1 = 0.593 nF, C2 = 1.98 nF, and n = 0.44. The value of the variable internal resistance, Rv is obtained from the following method.

When the load is open, the equivalent circuit at the resonance frequency is as in Fig. 4. Using fundamental approximation, the input impedance Zin is

$$|Z_{in}| = \frac{V_{1,rms}}{I_{1,rms}} = \left| \frac{1}{j\omega C_1} \| R_v \right| \qquad (2)$$

Then, the internal resistance, Rv is calculated by the following equation.

$$R_v = |Z_{in}| \frac{1}{\sqrt{1-(\omega |Z_{in}| C_1)^2}} \qquad (3)$$

This calculation is repeated through several input current levels from the measurement data. Using a curve fitting algorithm, f(.) is approximated as a third-order polynomial as in Fig. 5 and it is incorporated into the SPICE behavioral model. The SPICE behavioral model of the PT is constructed in Fig.6 employing this variable resistance. The model will be used in the ballast design in the next section. The flow chart for the model derivation sequence is summarized in Fig. 7.

Figure 8 compares measured and simulated open load voltage gain curve of the PT using the derived model at several input current levels. Figure 9 shows the comparisons of measured and simulated voltage gain of the PT as resistive load varies. It is shown that the derived model can be used in the voltage gain calculation for the design of ballast.

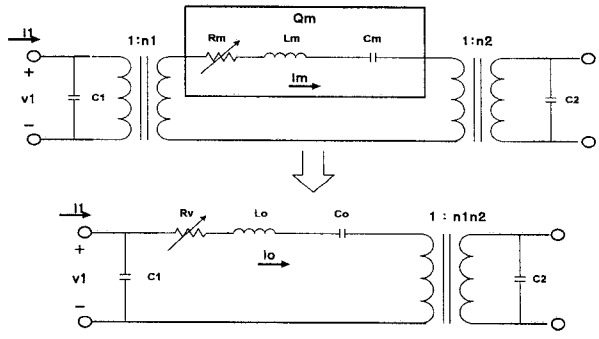

Fig. 3. Modified electrical equivalent model of PT

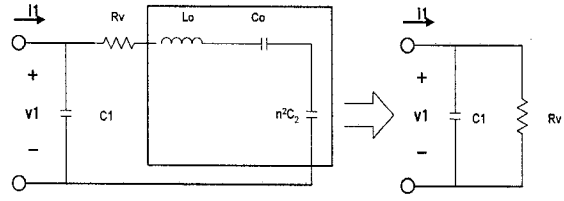

Fig. 4. Equivalent circuit at the resonance frequency with open load.

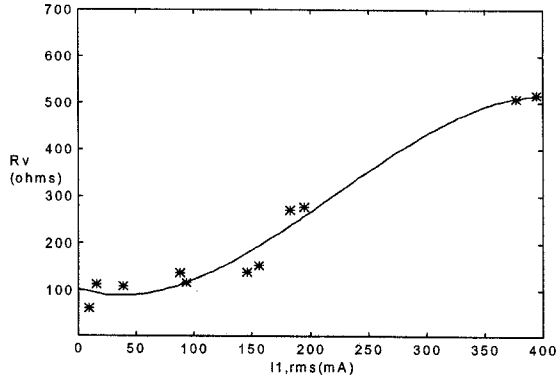

Fig. 5. Curve fitting for Rv

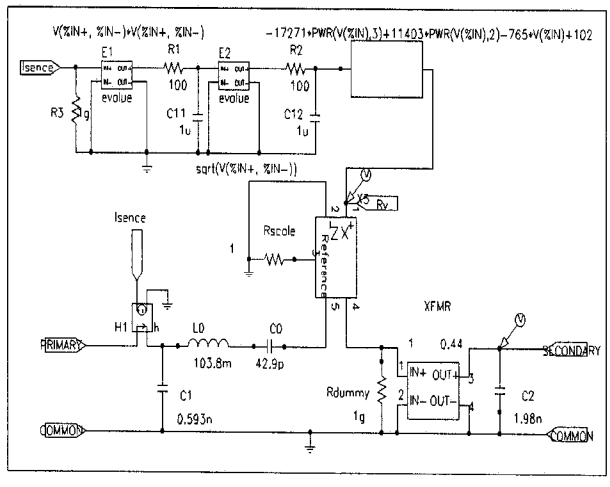

Fig. 6. SPICE behavioral model

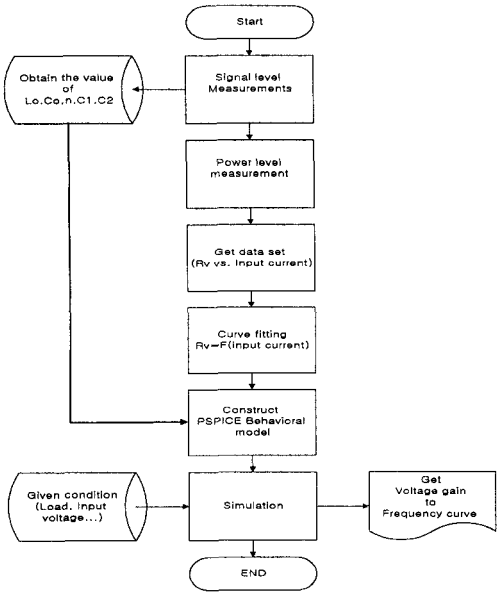

Fig. 7. Flow chart for the model construction

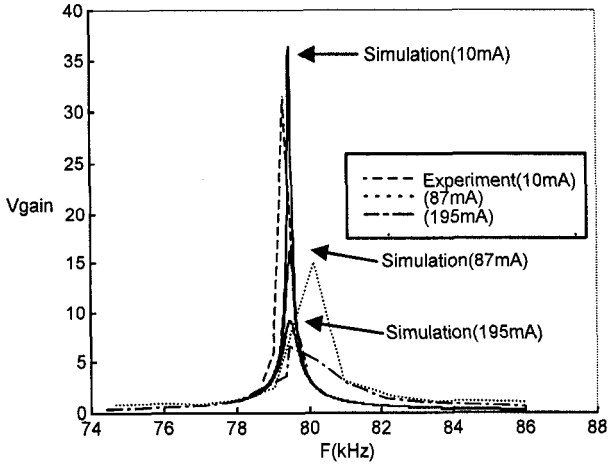

Fig. 8. Open load voltage gain at several current levels

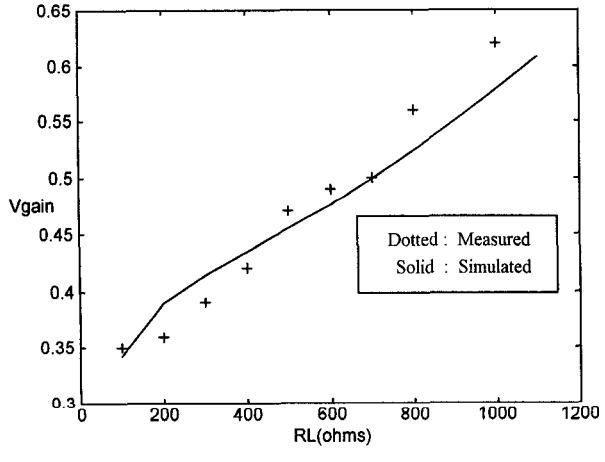

Fig.9. Maximum Voltage gain as resistive load varies

III. ELECTRONIC BALLAST USING THE PT

Generally, in the electronic fluorescent lamp (FL) ballast circuit, a resonant circuit such as the series-parallel or the half-bridge resonant topology as shown in Fig. 10 is used. The inductor (Lr) limits the current and resonates with the parallel capacitor (Cp) to provide lamp a sufficient starting voltage. However, this inductor raises the cost of the electronic ballast.

In this paper, to eliminate the magnetic component, FL ballasts using the PT in place of the inductor is suggested.

A. Low-power PT ballast

In Fig.11, a low power PT ballast circuit is presented. As mentioned in the previous section, the PT has a high voltage gain in the light load and a low voltage gain in the heavy load. This characteristic matches well with FL load. Before ignition, FL has no current path and is modeled by an open circuit. When it ignites, it behaves like a non-linear resistor[12].

When a square voltage waveform is applied to the primary part of the PT, from the inherent resonant characteristics, output waveform of the PT is sinusoidal as in Fig. 12. Also, the output voltage is dependent on the load impedance.

Cext provides the preheating current path to the rapid start FL. In order to provide a sufficient preheating current, Cext=2.2nF is used. Using the model developed in the previous section, the voltage gain curve is generated as shown in Fig.13. For the steady state operating condition a 12W equivalent lamp load of 800 ohms is used for the simulation. Before ignition, the starting voltage should be

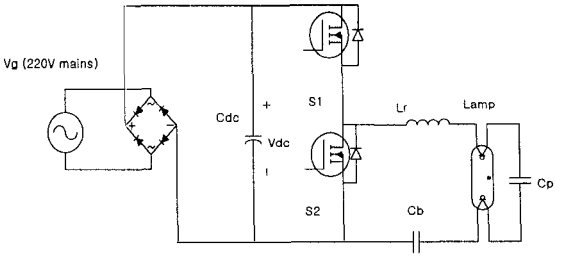

Fig.10. Conventional Ballast

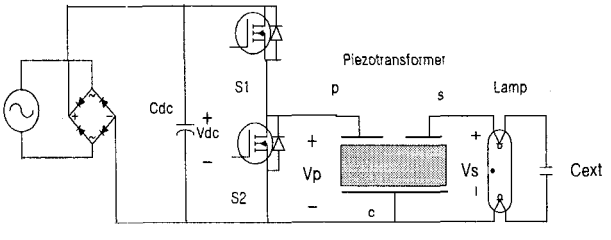

Fig. 11. Low power PT Ballast

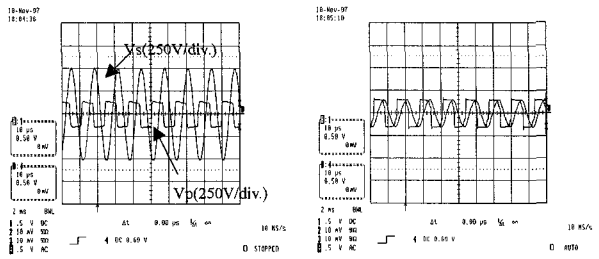

(a) before starting (b) after starting

Fig.12. PT gain curve

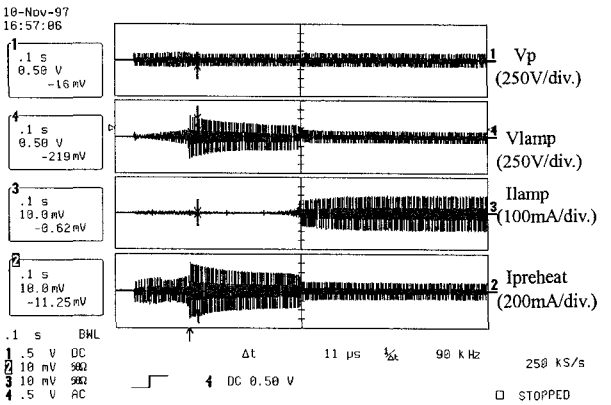

Fig.14. Starting behavior

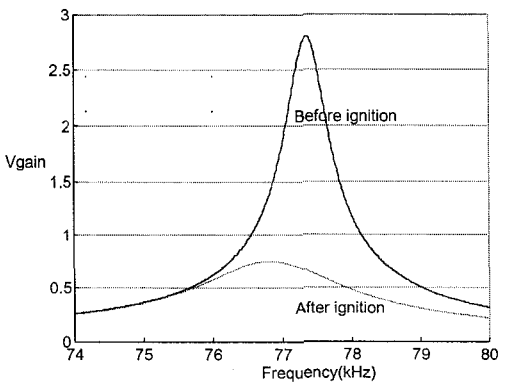

Fig. 13. Voltage gain curve with Cext=2.2nF

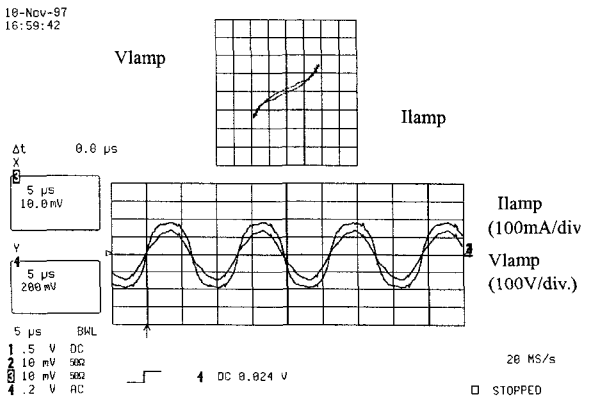

Fig. 15. 12.5W PT Compact FL Ballast

about 500Vpeak, whereas the steady state voltage of 100Vrms is needed. The voltage gain is calculated as follows;

$$V_{p,fund,rms} = 220 \times \frac{4}{\pi} \quad (4)$$

$$V_{gain,starting} \cong \frac{500/\sqrt{2}}{V_{p,fund,rms}} = 2.5 \quad (5)$$

$$V_{gain,s.s.} \cong \frac{100}{V_{p,fund,rms}} = 0.56$$

Therefore, from Fig.13, operating frequency of 77.2kHz is obtained.

Figure 14 is the starting behavior of the PT ballast with compact FL (OSRAM DULUX). It operates in the fixed operating frequency, and it does not provide the optimal preheat condition. It is, however, possible to improve the preheat condition by using the frequency control, as is used in the conventional ballast [13]. Figure 15 shows the steady state lamp current and voltage waveforms. Because of the high Q characteristics of the PT, the waveforms are near sinusoidal, and the crest factor of the lamp current is very low.

B. High-power PT ballast with charge pump PFC.

Nowadays, the increasing demand for the input line current regulation to meet the total harmonic distortion (THD) specification such as IEC 1000-3-2 is an important issue in the power electronics field. As the operating power increases, the electronic ballast may require the power factor correction (PFC).

Due to the input capacitance, C1 of the PT, when the square voltage waveform is directly applied to the PT, the high peak current flows through the switches, and for the reduction of this current a small inductor (Lr) is needed. This is especially necessary for a higher power ballast for which a multi-layer structure is adopted for the higher power capacity of PT. The inductor resonates with the PT input capacitor to produce the sinusoidal voltage waveform in the primary part of the PT. However, the input voltage of the PT increases too high, the isolation between the primary and secondary electrodes may be broken. For the sample used for this design, it is necessary to limit the driving voltage to Vdc, about 300V, by the diode clamp(D1 and D2) as shown in Fig. 16. The voltage waveforms of this driving circuit is in Fig. 17.

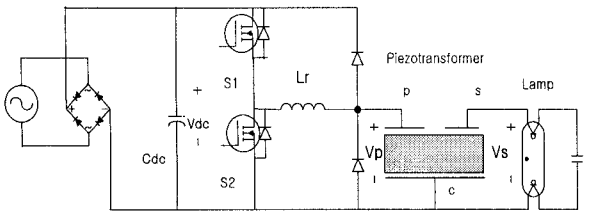

Fig. 16. Diode clamping technique in PT

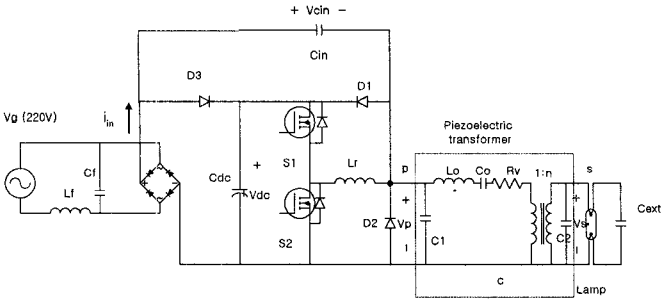

Fig. 18. Proposed Fluorescent Lamp Ballast with PFC

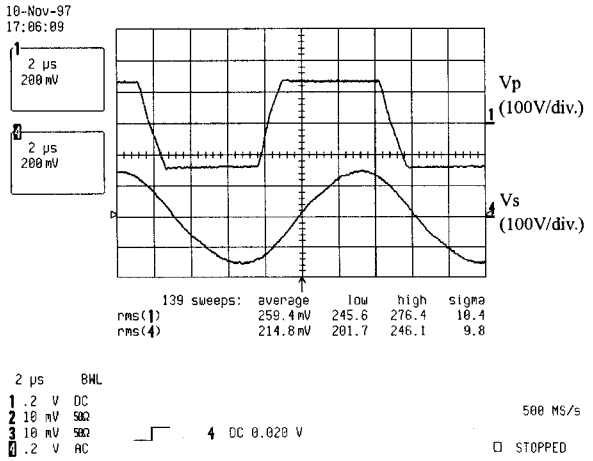

Fig.17. PT primary and secondary voltage waveforms

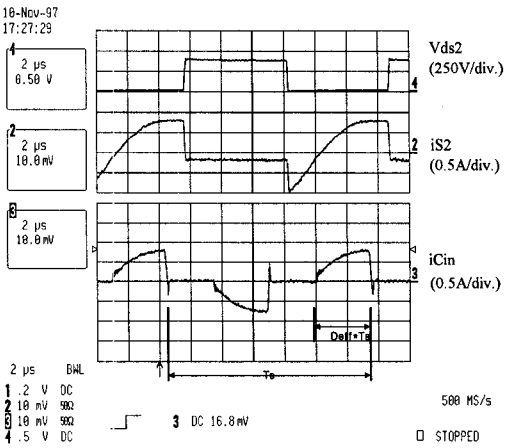

Fig.19. Waveforms of the charge pump PFC PT ballast

Figure 18 shows the diode-clamped PT ballast implemented to the charge pump PFC [7]. In the charge pump PFC circuit, average input current in one switching cycle equals the average charge current of Cin:

$$i_{in,avg} = f_s C_{in} \Delta Q_{ch} = f_s C_{in}(V_g + 2V_{p,mag} - V_{dc}) \quad (6)$$

where, Vp,mag is the peak voltage of the primary side of PT. Because the primary voltage Vp is clamped by diodes,

$$2V_{p,mag} = V_{dc} \quad (7)$$

therefore,

$$i_{in,avg} = f_s C_{in} V_g \quad (8)$$

This implies that input current has a good power factor and the magnitude of the Vp cannot affect the average input current. When using the charge pumping capacitor Cin with a conventional ballast such as a series-parallel inverter, there are some distortions in the output current, because Cin affects L-C resonant circuit. Therefore, some ballasts adopt the additional secondary resonance circuit [7]. However, in the proposed PT ballast, Cin is not a factor directly determining the PT output, i.e. lamp voltage, because lamp voltage is developed by the PT gain.

The design equations are derived using the power balance equation. The input power during the half line cycle has to be equal to output power. From (8), input power during the half line cycle is given by,

$$P_{in} = \frac{1}{\pi}\int_0^{\pi} i_{in,avg} v_g d\theta = \frac{P_{out}}{\eta} \quad (9)$$

$$f_s V^2_{g,rms} C_{in} = \frac{P_{out}}{\eta} \quad (10)$$

$$C_{in} = \frac{P_{out}/\eta}{f_s V^2_{g,rms}} \quad (11)$$

where, η is the circuit efficiency.

For the inductor Lr, the current through the inductor Lr is shown in Fig.19. Assume that Cin >> C1, the input current can be approximated by

$$i_{in} = \frac{|V_g|}{Z_o}\sin\omega_0 t \qquad (0 \le t \le D_{eff} T_s) \quad (12)$$

So, the average input current in one switching time is given by

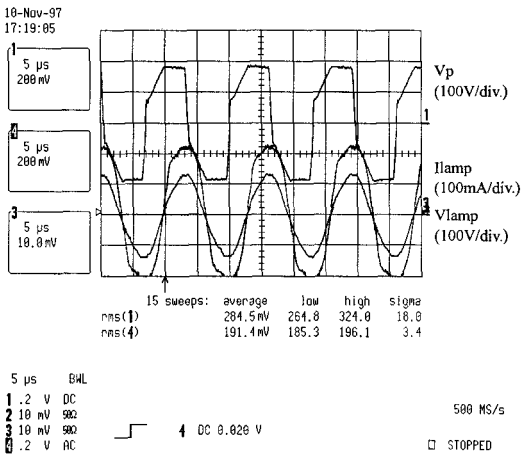

Fig.20. Waveforms of the charge pump PFC PT ballast

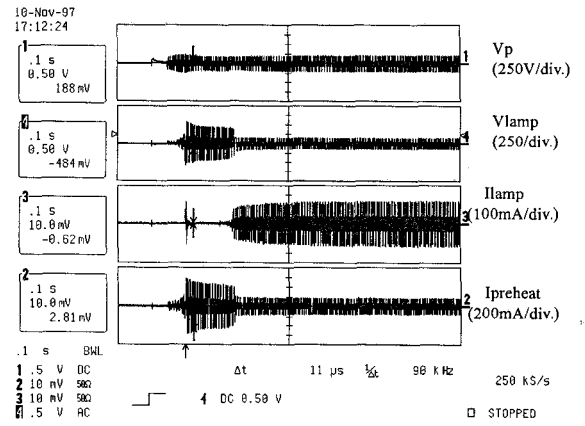

Fig. 22. Starting behavior

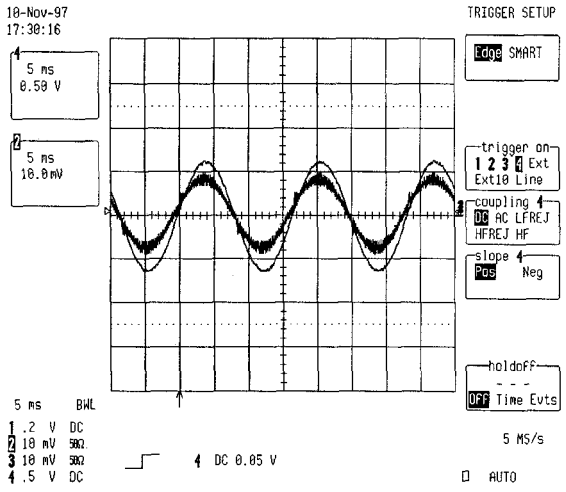

Fig. 21. Line current (200mA/div.) and line voltage(250V/div.)

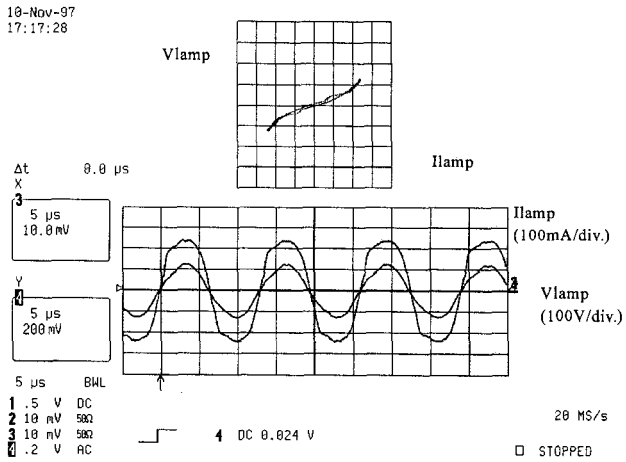

Fig. 23. Steady state lamp voltage and current

$$i_{in,avg} = \frac{1}{T_s}\int_0^{D_{eff}T_s}\frac{|V_g|}{Z_o}\sin\omega_0 t\,dt \qquad (13)$$

$$= \frac{|V_g|}{2\pi Z_o}(1-\cos 2\pi D_{eff})$$

where, $\omega_o = \frac{1}{\sqrt{L_r C_{in}}}$ $\quad Z_o = \sqrt{\frac{L_r}{C_{in}}}$

By equating (8) and (13), Lr is obtained as follows

$$L_r = \frac{(1-\cos 2\pi D_{eff})}{4\pi^2 C_{in} f_s^2} \qquad (14)$$

IV. EXPERIMENTAL RESULTS

The hardware experiments were carried out with a suggested charge pump PFC ballast for a compact fluorescent lamp (OSRAM Dulux EL 20W/21). The input line is from 220V mains and the operating frequency is fixed to 77.2kHz. Substituting fs=77.2 kHz, Deff=0.25, Po=18W, η=70%, Vp,mag $=\sqrt{2}$ x220V in the design equation, we obtain Cin=6.72nF, Lr=644uH.

Figure 20 shows the experimental waveforms. Figure 21 shows the waveforms of the line-input current and voltage of the ballast, where the power factor more than 0.99 is obtained. The starting behavior of the lamp is in Fig. 22, and the steady state lamp voltage and current in Fig. 23. From the figure, the current crest factor is very low. If the variable

frequency control scheme is used, it will also meet the preheating current specification.

V. CONCLUSION

The modified equivalent model of the PT considering the operating current level is derived to design of fluorescent lamp ballast. This model describes the voltage gain of the PT in wide load variations and various input current levels.

The FL ballasts using the PT are presented. The PT reduces the number of magnetic components and thus the cost. For low power ballasts, direct replacement of the resonant components by the PT is possible. For high power ballasts, the charge pump PFC FL ballast circuit using the PT is presented. This topology reduces the cost of the overall system.

The power capacity of the currently developed PT is relatively low (18W), but it can be increased by adopting a multi-layer structure and is currently under investigation. It is also possible to parallel the PT for higher power processing.

REFERENCES

[1] C.Y.Lin and F.C.Lee, "Piezoelectric transformer and its applications," Proc. of VPEC seminar, Sep., 1995.

[2] M. Shoyama, K. Horikoshi, T. Ninomiya, T. Zaitsu and Y. Sasaki, "Operational analysis of the push-pull piezoelectric inverter," IEEE APEC and Exposition, Feb., 1997, pp.573-578.

[3] T.Zaitsu, T.Inoue, O.Ohnishi, and A.Iwamoto, "2 MHz power converter with piezoelectric ceramic transformer," IEEE INTELEC '92 Proc., pp. 430-437, Oct.1992.

[4] T.Zaitsu, O. Ohnishi, T. Inoue, M. Shoyama, T.Ninomiya, F.C.Lee, and G.C.Hua, "Piezoelectric transformer operating in thickness extensional vibration and its application to switching converter," IEEE PESC Record, June, 1994.

[5] T. Zaitsu, T. Shigehisa, M. Shoyama, and T. Ninomiya, "Piezoelectric transformer converter with PWM control," IEEE APEC, 1996, pp. 279-283.

[6] C.Y.Lin and F.C.Lee, "Design of piezoelectric transformer converters using single-ended topologies," VPEC Power Electron. Sem. Proc.,1994.

[7] Wei Chen and F.C.Lee, "An improved charge pump electronic ballast with low THD and low crest factor," IEEE APEC, 1996, pp. 622-627.

[8] H.W.Katz, "Solid-state magnetic and dielectric devices," John Wiley & Sons, Inc., 1959.

[9] PJM Smidt and JL Duarte, "Powering neon lamps through piezoelectric transformers," IEEE PESC'96, June, 1996, Vol.2, pp.310-315.

[10] C.Y.Lin and F.C.Lee, "Design of a piezoelectric transformer converter and its matching networks," PESC Record, 1994, pp. 607-612.

[11] Yuichi Kaname and Yukihiko Ise, "A study of transducer design of piezoelectric ceramic transformers," The Journal of the Acoustical Society of Japan, Vol.32, No. 8, Aug., 1975.

[12] P.R.Herrick, "Mathematical models for high intensity discharge lamps," IEEE Transactions on industry applications, Vol. IA-16, NO. 5, Sep./Oct., 1980.

[13] Y. Ji and R. Davis, "Starting performance of high-frequency electronic ballasts for 4-foot fluorescent lamps," IAS Annual Meeting, Vol. 3, Oct., 1995, pp. 2083-2089.